Improved mitigation of self-phase modulation induced impairments in 28 GBaud phase-sensitive amplified links

Research Article | Vol. 27, No. 4 | 18 Feb 2019 | OPTICS EXPRESS 4304
Optics EXPRESS

Improved mitigation of self-phase modulation induced impairments in 28 GBaud phase-sensitive amplified links

EGON ASTRA,[1,*] HENRIK ELIASSON,[2] TOOMAS RUUBEN,[1] AND PETER A. ANDREKSON[2]

[1] *Thomas Johann Seebeck Department of Electronics, Tallinn University of Technology, Tallinn, Estonia*
[2] *Department of Microtechnology and Nanoscience, Photonics Laboratory, Chalmers University of Technology, Göteborg, Sweden*
[*] *egon.astra@ttu.ee*

Abstract: The improved mitigation of self-phase modulation (SPM) induced nonlinear impairments by the use of a multi-span dispersion map optimization in 28 GBaud phase-sensitive amplifier (PSA) links is numerically investigated. We show that a four-span dispersion map optimized PSA link provides 2.1 times reach improvement over a single-span optimized PSA link with a total nonlinear phase shift tolerance increase from 2.1 radians to 8.8 radians. Furthermore, the optimized PSA link increases the maximum transmission reach by 6.9 times compared to a single-span optimized in-line dispersion managed phase-insensitive amplifier (PIA) link and 4.3 times reach extension is achieved compared to a dispersion unmanaged PIA link.

1. Introduction

Phase-sensitive amplifiers (PSAs) are known for their ability to increase transmission system performance [1, 2], mainly limited by amplifier noise and fiber nonlinearities in fiber-optic links [3–5]. This is possible due to the combined ultra-low noise amplification and nonlinearity mitigation capability of PSAs [2, 6]. PSAs quantum-limited noise figure (NF) is 0 dB [7, 8] and a NF of 1.1 dB has been reported in experiments [9, 10]. In contrast, conventional phase-insensitive amplifiers (PIAs) have a quantum-limited NF of 3 dB [7]. A recent experimental study showed 5.6 times transmission reach improvement by using PSAs instead of PIAs such as erbium-doped fiber amplifiers (EDFAs) in an in-line dispersion managed 10 GBaud fiber-optic link that could tolerate a total accumulated nonlinear phase shift of 6.2 radians [11].

The nonlinearity mitigation effect in a frequency non-degenerate two-mode (signal and it's phase conjugated wave, called the idler, at different wavelengths [12]) PSA link is similar to the nonlinearity mitigation of a phase-conjugated twin-wave (PCTW) approach, where signal and idler waves can be transmitted on different polarizations, wavelengths or time-slots [13–15]. Signal and idler waves are both co-propagated through a nonlinear transmission medium, where they experience nonlinear distortions during propagation. The nonlinearity mitigation is performed in a coherent superposition (CS) process where a signal wave and an idler wave, that is phase conjugated again during the process, are coherently superposed. In a PSA link, the CS is performed during a parametric phase-sensitive amplification process by a PSA, where correlated phase distortions on signal and idler waves are converted into smaller amplitude distortions, resulting in a phase-to-amplitude distortion conversion and a self-phase modulation (SPM) mitigation [2].

After the introduction of electronic dispersion compensation (EDC), coherent fiber optic links with in-line dispersion compensation were outperformed by EDC links without in-line dispersion management [16, 17]. However, PSA links need in-line dispersion management to fulfill the phase-matching criteria for a phase-sensitive amplification process [2]. Much work

#349310 https://doi.org/10.1364/OE.27.004304
Journal © 2019 Received 29 Oct 2018; revised 12 Dec 2018; accepted 15 Dec 2018; published 6 Feb 2019

Optics EXPRESS

regarding the dispersion map optimization for in-line dispersion compensated PIA links has been carried out [18–20], but these principles are not directly applicable to PSA links, since the effectiveness of the nonlinearity mitigation in PSA links is highly dependent on correlation properties of propagated signal and idler waves. It has been shown previously that the dispersion management for a single-span dispersion map optimized PSA link [2, 11, 21] and for a two-span dispersion map optimized PSA link [22] plays an important role for the nonlinearity mitigation performance. The importance of dispersion map optimization for twin-waves was first noted in [13], where according to the first-order perturbation theory, a symmetric span power map with an anti-symmetric dispersion map should be used for the best nonlinearity mitigation performance for the PCTW approach. In [23] it was experimentally shown that 50% dispersion pre- and post-compensation for a Raman assisted PSA link with almost power-symmetric fiber spans results in an increased nonlinearity mitigation performance. However, in our study, PSA links with lumped amplification are under investigation and therefore different dispersion map optimization assumptions have to be used.

In [24], it was shown numerically that the nonlinearity mitigation performance of a 28 GBaud PSA link can be significantly increased by allowing different span dispersion maps to be used in a multi-span dispersion map optimization. A dispersion map was optimized up to four spans with a dispersion compensation value step precision of 5% that resulted in 2.1 times PSA transmission system maximum reach increase compared to a single-span optimized PSA link. In this paper, we investigate by numerical simulations a 28 GBaud PSA link dispersion map optimization up to four spans with an optimization step precision of 1% and compare these results with 5% optimization precision results in a long-haul transmission. Furthermore, the dispersion map optimized PSA link maximum long-haul transmission reaches are compared with conventional EDFA long-haul transmission link maximum reaches with dispersion in-line compensated and in-line uncompensated EDC links. The SPM mitigation is also investigated for a wavelength-division multiplexing (WDM) system scenario where the wavelength separation between signal and idler waves increases with the increasing number of channels, therefore resulting in increasingly different dispersion parameter values for signal and idler wavelengths.

2. General simulation model

The simulation model that was used is shown in Fig. 1. The model consists of a transmitter, N PSA or PIA amplified and dispersion-managed transmission spans and a receiver. At the transmitter, a 10 GBaud or 28 Gbaud quadrature phase-shift keying (QPSK) modulated signal S was generated. The generated signal waveform was a non-return-to-zero (NRZ) signal oversampled to 32 samples per symbol and filtered with a 5th order Bessel filter characteristic with 75% full width half maximum (FWHM) bandwidth of the used symbol rate. In all simulations single-channel and single-polarization signals were used. After the signal waveform generation, the signal was divided between upper and lower path, where the latter was used to generate the idler I through an ideal conjugation of the signal $I=S^*$ if a PSA implementation was desired. No wavelength conversion in the conjugation process was made, as signal and idler waves were separately propagated assuming a 8 nm wavelength separation. Separate propagation was used to neglect inter-channel nonlinear effects between signal and idler channels and to focus only on the PSA performance of mitigating the SPM effects. The launch powers P_{in} of signal and idler were set by an ideal and noiseless amplification before they were launched into the transmission span. The launch power is given per signal and per idler, resulting in a 3 dB higher total launch power.

After the waveforms were launched into the transmission span, they were dispersion pre-compensated before and post-compensated after each standard single mode fiber (SSMF) in the dispersion compensating modules (DCMs) by values $D_{\text{pre,n}}$ and $100\% - D_{\text{pre,n}}$ meaning that each span was fully dispersion compensated. The simulated DCMs were ideal (linear and lossless). The index n shows span number, where N is the total number of spans in the

Optics EXPRESS

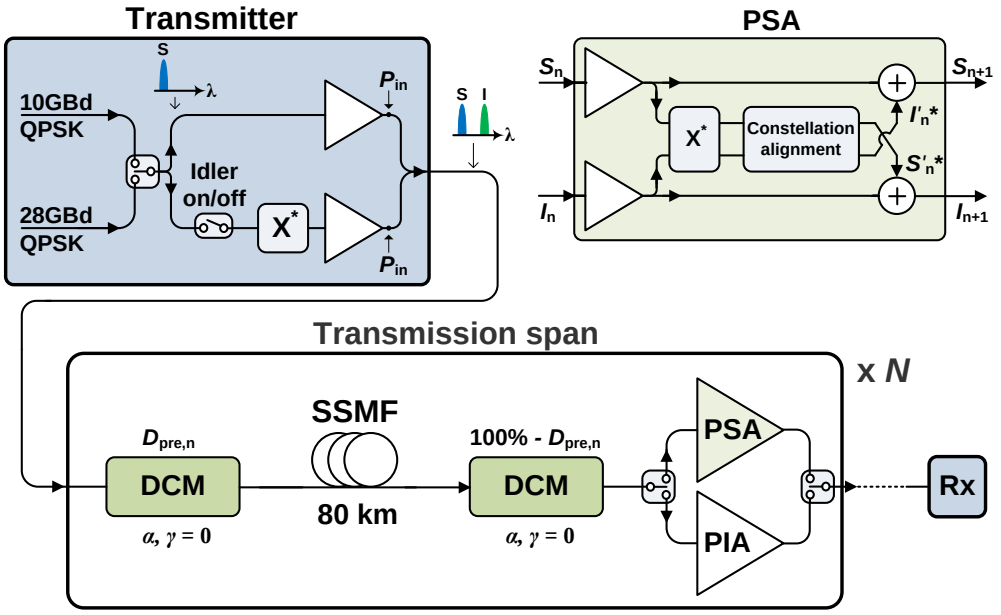

Fig. 1. The simulation model for a PSA or a PIA amplified transmission link. Acronyms are explained in the text.

transmission link and n=1...N. The simulated SSMF length was 80 km. The SSMF parameters were loss α = 0.2 dB/km, dispersion parameter D = 17 ps/nm/km and nonlinear coefficient γ = 1.27 $W^{-1}km^{-1}$. The propagation of light in the SSMF was modeled by using two separate (for signal and idler waveform) split-step Fourier method (SSFM) solutions of the nonlinear Schrödinger equation (NLSE). For simplicity and better understanding, the used group velocity dispersion (GVD) parameter β_2 was same for signal and idler waves, if not stated otherwise. In [2] and [22] it is noted that different GVD parameter value for a 8 nm wavelength separation does not have significant impact on the SPM induced nonlinearity mitigation performance of a PSA link.

At the end of each transmission span, the loss of the transmission span was compensated by PSA or PIA amplification. The in-line amplifiers used in the simulations were ideal and noiseless, unless it is stated otherwise by the given NFs. The phase-sensitive amplification process was modeled using a simplified model, shown in Fig. 1, under the assumptions that the PSA was operating in a high-gain regime with low signal input powers [2, 6]. The signal S_n and idler I_n are both amplified by the gain necessary to compensate the span loss and then separated for conjugation and constellation alignment processes. As a result of the constellation alignment process, constellations of the conjugated signal S_n* and idler I_n* are rotated by introducing the necessary phase-shift to maximize the power after coherent addition of signal S_n and conjugated and rotated idler I'_n* in the upper arm and coherent addition of idler I_n and conjugated and rotated signal S'_n* in the lower arm resulting in a phase-sensitively amplified signal S_{n+1} and idler I_{n+1} waveforms. The transmission span amplifier noise was added only in the long-haul simulations with a PSA NF=1.1 dB [9] to signal and idler and a 3 dB higher NF=4.1 dB was used for PIA case [7, 8]. In the PSA simulation model, the uncorrelated additive Gaussian noises were added to signal and idler waves in the amplification stage at the PSA model input shown in Fig. 1, by following a general output noise formula of a PSA that is based on semi-classical theory of quantum mechanical system under the high-photon-number assumption described in [25]. For

Optics EXPRESS

all of the other simulations, no amplifier noise was added in order to avoid unwanted nonlinear phase noise (NLPN) effects. It should be noted that also the effects of laser phase noise and polarization were neglected in all simulations to only observe the impact of the dispersion map on the efficiency of the mitigation of SPM induced nonlinear distortions.

After N transmission spans, the signal waveform was detected in the receiver Rx for error vector magnitude (EVM) [26] or bit error ratio (BER) estimation. A conventional receiver for detecting QPSK signals was used, consisting of a down-sampler to 2 samples per symbol, a channel equalizer deploying constant modulus algorithm (CMA) and the Viterbi-Viterbi phase recovery algorithm to align constellation for EVM or BER calculations.

3. 28 GBaud QPSK PSA link dispersion map optimization

3.1. Dispersion map optimization procedure

The dispersion map optimization was carried out for one, two, three and four-span 28 GBaud QPSK PSA links. In this paper, the optimized dispersion pre-compensation values were found with a precision of 1% and compared with values from a 5% optimization precision procedure that was presented in [24]. For the optimization procedure, PSA links with different dispersion map configurations were simulated. The dispersion map configuration is determined here by the dispersion pre-compensation value, that is swept and the post-compensation value is automatically adjusted assuming that transmission span is 100% dispersion compensated. As a result of the simulation, an EVM metric was calculated and the dispersion map configuration of a PSA link with the lowest EVM value was selected as an optimal solution. The signal launch power was set to 9 dBm for all cases to assure a sufficient EVM level for comparison.

For the one-span PSA link optimization procedure, the dispersion pre-compensation value was swept from -20% to 80% resulting in 101 dispersion map scenarios with an optimization step accuracy of 1%. For a two-span PSA link, the dispersion pre-compensation value for the span one was swept from -40% to 40% and for the span two from 0% to 80%, resulting in 6561 dispersion map scenarios. For the three-span case, coarse sweeps with a precision of 2% were performed over total range of -40% to 100% to estimate the best regions for fine sweeps. The final sweep with 1% precision was performed from -20% to 0% for the span one, 10% to 30% for the span two and 42% to 62% for the span three, resulting in 9261 dispersion maps. Also for the four-span optimization, coarse sweeps with a precision of 5% and 2% were first performed over total range of -40% to 100% to find the best sweep regions for fine sweeps. Also the fine sweeps with 1% precision were performed over multiple sweep ranges where a sweep for a span consisted of 11 points resulting in 14641 dispersion maps for one optimization sweep run of four-span optimization.

It should be noted that it is possible that the found optima for three and four-span optimization are local optima and we cannot claim for certain that we have found the global optimum, since sweep ranges of a dispersion map optimization are restricted. However, by brute forcing simulations for three and four-span PSA link dispersion map optimization over large sweep areas for every span leads to an unrealistic computational effort. For example a four-span optimization with a 1% precision over a range of -20% to 80% for all the four spans, results in over 104 million different dispersion map configurations.

3.2. Dispersion map optimization results

The comparison between 5% and 1% optimization step precision of one to four-span dispersion map optimization at a signal launch power of 9 dBm is shown in Fig. 2(a). The 1% precision optimized dispersion maps compared to the 5% optimized maps show clear EVM improvement with every number of dispersion map optimized spans. In fact the 1% optimization precision for the four-span dispersion map optimized case is 0.3 dB better in terms of EVM than in 5%

Optics EXPRESS

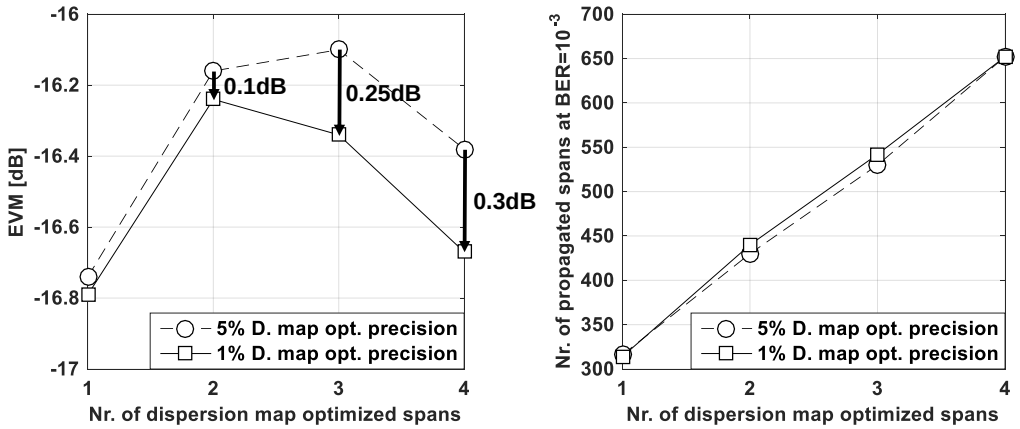

Fig. 2. Simulation results showing (a) EVM performance comparison of 5% and 1% optimization precision at a signal launch power of 9 dBm and (b) maximum number of propagated spans at BER = 10^{-3} at optimal launch power comparison between PSA dispersion map optimization precision steps of 5% and 1% as a function of number of dispersion map optimized spans.

steps optimized dispersion map case. Furthermore the four-span optimized dispersion map case with an optimization precision of 1% results in a significant nonlinearity mitigation performance where the signal quality in terms of EVM after a propagation of four spans is only 0.15 dB worse than the best scenario for single-span PSA link. It means that the PSA link reach can be fourfold increased for a fixed launch power in a highly nonlinear regime if four-span optimized dispersion maps are used.

Despite the short-haul links with a 1% optimization precision step up to four span optimization show improved results, it turns out that in long-haul propagation studies (see simulation details in section 4), these dispersion map optimized links show no significant improvement with the higher optimization precision. Figure 2(b), where dispersion map optimized spans for 1% and 5% optimization precision are used repeatedly at optimal launch powers, shows that a 1% precision in a dispersion map optimization does not increase the maximal PSA link reach with four-span optimized case. The maximum number of propagated spans with a four-span optimization at BER = 10^{-3} is 652 spans for the both optimization precision cases. However, a slight improvement less than 2.3% for a 1% optimization precision can be seen for the two and three-span optimization cases. The two-span case propagation distance is increased from 430 spans to 440 spans and for the three-span optimization case increase is from 531 spans to 543 spans. It is possible that the nature of the EVM metric can hinder the optimization procedure since nonlinear distortions are not Gaussian distributed. An optimization procedure has also been performed (not shown here) by using the EVM measure only in phase or only in amplitude dimension, but no better optima were found. The usage of the EVM in phase dimension led to the same optimization results as the standard EVM measure. Secondly, the chosen launch power for the optimization was high compared to optimal launch powers that could cause an offset as the dispersion map optimum is slightly power dependent. However the launch power was kept at 9 dBm to ensure the reliability of the EVM metric.

In Fig. 3(a) with a 5% optimization precision and in Fig. 3(b) with a 1% optimization precision dispersion pre-compensation values are shown for the one to four-span optimized dispersion

Optics EXPRESS

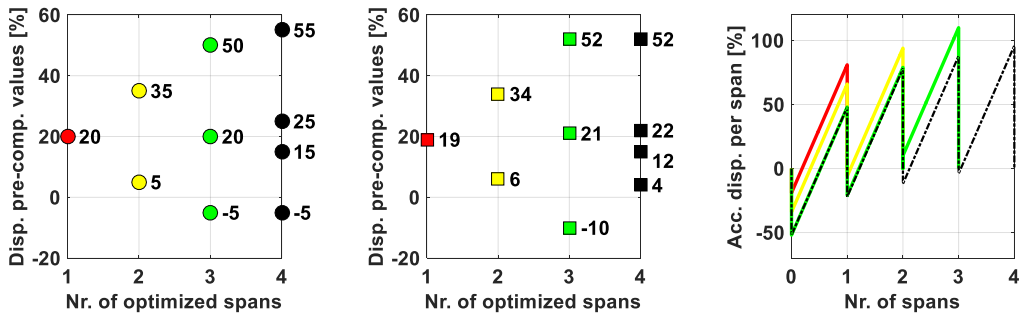

Fig. 3. Dispersion pre-compensation values for one to four-span dispersion map optimized PSA links in (a) 5% and (b) 1% optimization step precision, (c) dispersion maps corresponding to 1% optimization precision for one (red line), two (yellow line), three (green line) and four-span (black dashed line) dispersion map optimized PSA links.

map cases. Figure 3(b) shows that for the one to three-span optimized dispersion map cases with a 1% optimization precision, the dispersion pre-compensation values are expanding more symmetrically than for the 5% optimized case in Fig. 3(a). The opposite is true for the four-span optimized case where the 1% precision case loses its symmetrical and expanding trend compared to the 5% optimized case. However, the 5% and 1% optimized cases perform equally well based on the long-haul transmission simulation results, which show us that multiple dispersion map solutions are available for four-span optimized cases that can have an equal performance. That is not true for one to three-span optimizations where only the one optimum with given dispersion pre-compensation values in Fig. 3(b) is available regardless of the chosen order of dispersion pre-compensation values. It must be noted, that we have not observed (results not shown here) any significant performance difference of short-haul and long-haul simulations if the ordering of dispersion pre-compensation values is altered. Figure 3(c) shows the accumulated dispersion as a function of propagated distance in spans for all the four dispersion map optimization cases with 1% optimization step precision.

This non-improvement of the four-span optimization with a higher optimization step accuracy can lead to a false conclusion that arbitrary values can be chosen for four-span dispersion maps without losing link performance. Figure 4(a) shows an example of the dispersion pre-compensation values for the four-span dispersion map (gray boxes), chosen by following the symmetric and expanding nature of the one to three-span dispersion map optimized values. Figure 4(b) shows the long-haul simulation results comparing the link performances of the chosen dispersion map to the dispersion map optimized PSA link case at BER = 10^{-3}. The long-haul results in Fig. 4(b) show that the performance of the chosen dispersion map drops significantly compared to the optimized case, resulting in a maximum transmission distance of 546 spans that has approximately only the same reach as a three-span optimized long-haul PSA link at BER = 10^{-3}.

4. Long-haul 28 GBaud transmission comparison of dispersion map optimized PSA and PIA links

Long-haul simulations were performed to compare the maximum transmission distances at BER = 10^{-3} with optimum launch powers for one, two, three and four-span dispersion map optimized PSA links, an in-line dispersion compensated PIA link and a dispersion unmanaged PIA link with EDC as benchmarks. The dispersion unmanaged PIA link with EDC means

Optics EXPRESS

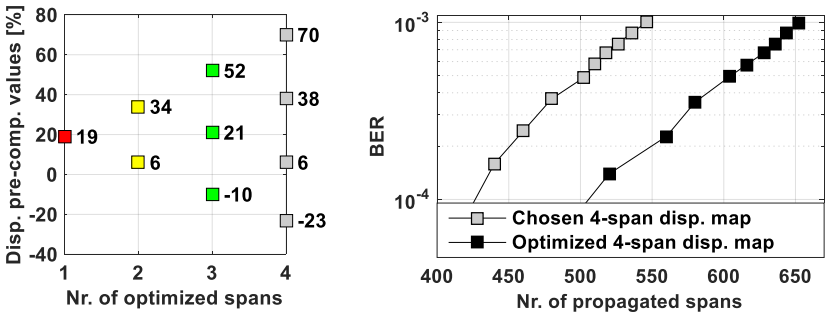

(a) (b)

Fig. 4. (a) Dispersion pre-compensation values up to four-span dispersion map optimized PSA links where the dispersion pre-compensation values for the four-span dispersion map case (gray boxes) are chosen by following the symmetric and expanding nature of the one to three-span dispersion map optimized values and (b) BER simulations comparing the long-haul performance of optimized and chosen PSA four-span dispersion map cases.

that the dispersion compensation is unmanaged inside the transmission link, but the dispersion pre-compensation is applied before the link in the transmitter and the post-compensation after the link in the receiver. We chose a NF of the PIA of 4.1 dB, which is about 1 dB larger than what is achievable in practice (quantum limit being 3 dB), while a NF of 1.1 dB was chosen for the PSA. In this way our simulations reflect the 3 dB NF difference in the quantum limit [7, 9], while at the same time reducing the computational effort. We expect that the relative differences between PIA and PSA will still be very similar, compared with a case of using 3 dB and 0 dB NFs, respectively. The dispersion pre-compensation values for an in-line dispersion compensated PIA link have been chosen according to the single-span dispersion map optimized PIA link, that is 15% dispersion pre-compensation and 85% post-compensation in every span. For the EDC PIA case, 50% of all the link accumulated dispersion was pre-compensated before a fiber transmission and 50% of accumulated dispersion was post-compensated after the last span [27, 28].

In Fig. 5 the maximum transmission reaches are shown for PSA and PIA links. The maximum transmission distances of PSA links for one, two, three and four-span dispersion map optimized cases are 316, 440, 543 and 652 spans respectively and for the in-line dispersion compensated PIA link 94 spans and for the PIA EDC link 150 spans at BER = 10^{-3}. The transmission reach of a PSA link can be improved approximately 2.1 times if four-span optimized dispersion maps are used repeatedly instead of a single-span optimized dispersion management throughout the transmission link. It is estimated up to four-span optimization that the improvement factor from multi-span dispersion map optimization is approximately equal to the square-root of the optimized span number, because the increase factors are 1.4, 1.7 and 2.1 for two-, three- and four-span optimized cases respectively compared to single-span optimized PSA case.

A significant transmission distance improvement of approximately 6.9 times is achieved by using a four-span optimized PSA link instead of a single-span optimized and dispersion in-line managed PIA link. However, the latter comparison is not entirely fair as PIA links without in-line dispersion management using EDC are more resilient to nonlinear impairments as can be seen in Fig. 5. That results in 4.3 times maximum transmission distance improvement if a four-span dispersion map optimized PSA link is used instead of a PIA EDC link. It must be noted that we have used ideal DCMs in our simulations for PSA links, but in reality DCMs will add loss and cause additional penalties e.g. due to nonlinearities and non-ideal phase response [29, 30]. Furthermore dispersion unmanaged PIA links with EDC do not require DCMs at all. However, we expect that the maximum transmission reach of a PSA link can be extended further if the

Optics EXPRESS

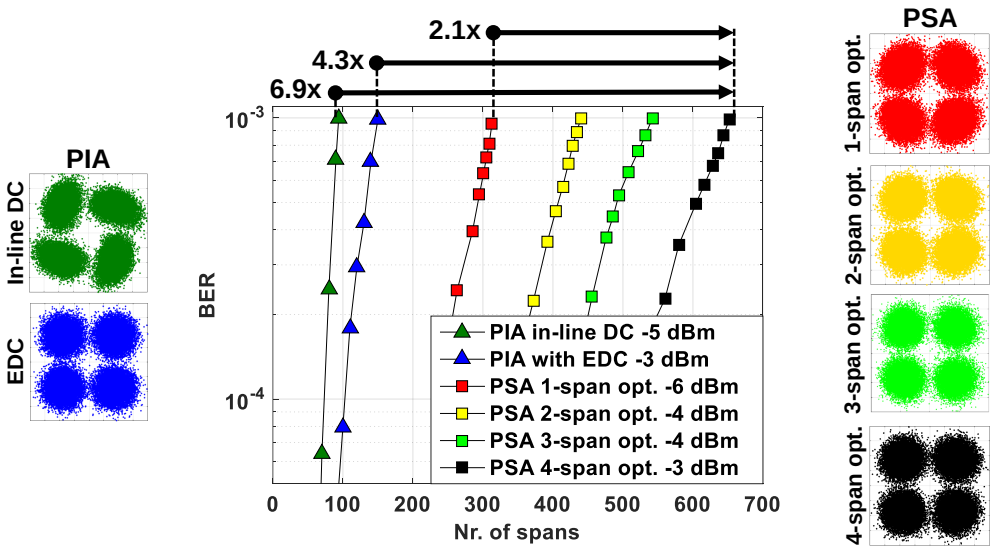

Fig. 5. Long-haul simulation results showing the BER vs. number of propagated spans and constellation diagrams at BER = 10^{-3} for one to four-span dispersion map optimized PSA links and EDFA links with and without an in-line dispersion compensation at optimum launch powers.

dispersion map over more than four spans is optimized.

The constellations are also shown in Fig. 5 for corresponding PSA and PIA links at BER = 10^{-3} level. The in-line dispersion compensated PIA link constellation is the most nonlinearly distorted. Nonlinear characteristics are also more visibly distinguishable for the one-span dispersion map optimized PSA link case than for the four-span optimized case. The four-span dispersion map optimized PSA link constellation is similar to constellation of PIA EDC link without any observable nonlinear characteristics. Using a four-span dispersion map optimized PSA link instead of a single-span optimized link, results in a maximum nonlinear phase shift tolerance fourfold increase from 2.1 radians to 8.8 radians or compared to a two-span optimized link, a maximum nonlinear phase shift tolerance increase from 4.7 radians to 8.8 radians.

5. Necessity of multi-span dispersion map optimization

It has been experimentally shown that a single-channel and single polarization two-mode PSA link at lower transmission speeds, such as 10 GBaud, can result in a remarkable transmission distance improvement of 5.6 times if a PSA link is used instead of an in-line dispersion managed PIA link [11]. However, our simulation study shows that at higher transmission speeds, such as 28 GBaud, a PSA ability to provide a significantly better transmission performance compared to a PIA link in a single-span transmission scenario, does appear to not hold anymore. Figure 6 shows 10 GBaud and 28 GBaud single-span transmission link performance improvements in terms of EVM, if a single-span PSA link is used instead of a single-span PIA link. The single-span optimized dispersion pre-compensation values were used 22% for a PIA and 24% for a PSA case at 10 GBaud and 16% for a PIA and 19% for a PSA case at 28 GBaud. At a symbol rate of 10 GBaud, where the dispersion length is much longer than the span length ($L_D \gg L_{span}$), a PSA link provides approximately 12 dB better EVM performance than a PIA link at 6 dBm signal launch powers. At 28 GBaud, when $L_D < L_{span}$, the improvement by using PSA link instead of a PIA link has diminished by 9.4 dB to a level of 3 dB. This improvement degradation at

Optics EXPRESS

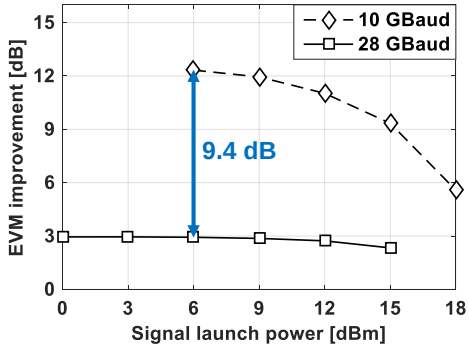

Fig. 6. EVM improvement as a function of signal launch power showing the improvement of using a single-span dispersion map optimized PSA link instead of a PIA link in terms of EVM for 10 GBaud and 28 GBaud single-span transmission links.

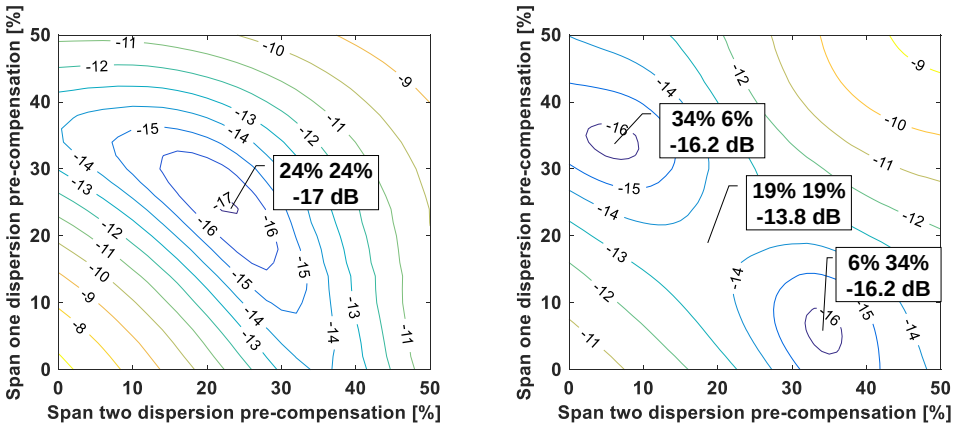

Fig. 7. Two-span dispersion map optimization simulation results showing EVM as a function of dispersion pre-compensation values for span one and span two for (a) 10 GBaud PSA link at 15 dBm launch power and (b) 28 GBaud PSA link at 9 dBm launch power.

higher symbol rate was also observed in [31], where distributed Raman amplified PSA and PIA links were experimentally compared. The improvement in Fig. 6 also degrades at higher launch powers where nonlinear distortions on signal and idler waves become less correlated.

Furthermore, in Figs. 7(a) and 7(b) are shown two-span dispersion map optimization results for 10 GBaud PSA link at 15 dBm launch power and 28 GBaud PSA link at 9 dBm launch power respectively. Figure 7(a) shows that there is an optimal solution by using the same dispersion pre-compensation value 24% for each span of a two-span 10 GBaud PSA link. The opposite is true for a two-span 28 GBaud PSA link where an optimal solution is to use a 6% dispersion pre-compensation in the first span and a 34% dispersion pre-compensation in the second span or vice versa. The improvement of using a two-span optimized case (6%, 34%) instead of using the same dispersion pre-compensation values in each span (19%, 19%) is 2.4 dB in terms of EVM. Therefore the multi-span dispersion map optimization for PSA links in condition where $L_D < L_{span}$ is of practical interest to fully utilize the PSA nonlinearity mitigation ability.

Optics EXPRESS

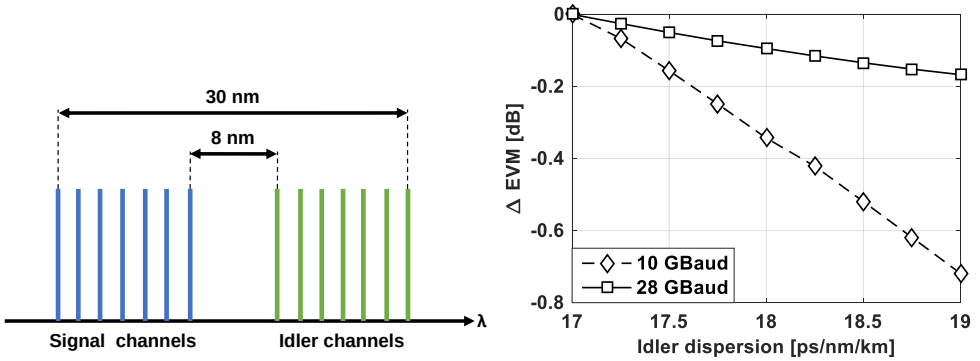

(a) (b)

Fig. 8. (a) An example of allocation of wavelengths between signal and idler channels in a WDM PSA system and (b) EVM change as a function of the idler dispersion parameter value showing the EVM difference if an idler dispersion parameter value is swept from 17 ps/nm/km and a signal dispersion parameter value is kept fixed at 17 ps/nm/km for 10 GBaud and 28 GBaud single-span PSA links at 9 dBm launch power.

6. Effect of third-order dispersion on SPM mitigation

In [2] and [22] it was claimed that the third-order dispersion effects do not play a significant role in a PSA nonlinearity mitigation performance and a simplification can be made to use the same GVD parameter for signal and idler waves. Therefore in our previous simulations this simplification was applied, although the signal and idler wavelengths are assumed to be 8 nm separated resulting in dispersion parameter values of D = 17 ps/nm/km for a signal and D = 17.56 ps/nm/km for an idler with a dispersion slope parameter approximately S = 0.07 ps/nm^2/km.

Nevertheless no exact indication or measure was given about the third-order dispersion effects. However, simulation results from section 5 showed that the dispersion length L_D plays a significant role in the SPM induced nonlinearity mitigation in a PSA link. Therefore we are interested also to benchmark the influence of signal and idler wavelength separation for 10 GBaud and 28 GBaud single-span PSA links as a function of a dispersion parameter change for an idler wave. Furthermore, in WDM PSA systems where signal and idler wavelengths are spaced more far apart with every added WDM channel, shown in Fig. 8(a), SPM mitigation is also of practical interest, since PSA amplification is WDM compatible [32–34].

Simulations were performed where the third-order dispersion effects were included and the PSA link SPM mitigation performance regarding the idler wavelength separation up to 30 nm were investigated. The signal dispersion parameter value was kept fixed at D = 17 ps/nm/km and the idler dispersion parameter value was swept from D = 17 ps/nm/km to D = 19 ps/nm/km corresponding to a wavelength separation of signal and idler waves from 0 nm to 30 nm. Due to different accumulated dispersion values on signal and idler waves, the dispersion compensators used in these simulations were capable of compensating for the dispersion slope as well. The results are shown in Fig. 8(b), where the measure of influence is conveyed in terms of EVM difference taken from the EVM value where the signal and idler waves have 0 nm wavelength separation.

Figure 8(b) shows that a 28 GBaud single-span PSA link is more resilient to third-order dispersion effects than a 10 GBaud PSA link. In fact, the used 8 nm wavelength separation, where the idler dispersion parameter value is D = 17.56 ps/nm/km, has a very small offset of approximately 0.05 dB in terms of EVM for the 28 GBaud PSA link, but more significant

Optics EXPRESS

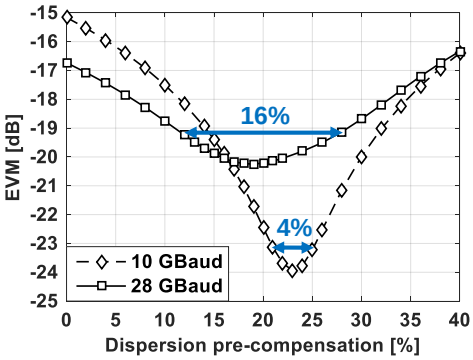

Fig. 9. EVM as a function of applied dispersion pre-compensation showing the chosen dispersion map dependence on a link performance for 10 GBaud at 12 dBm launch power and 28 GBaud at 6 dBm launch power single-span PSA links.

difference nearly 0.2 dB for the 10 GBaud single-span PSA link. If the signal and idler separation is 30 nm for the 10 GBaud PSA link, then the PSA's SPM mitigation results in an approximately 0.7 dB worse EVM performance.

The resiliency of the 28 GBaud PSA link can be related to the fact that in a condition where $L_D < L_{span}$, the dispersion itself plays major role reducing the twin-wave nonlinearity mitigation efficiency. It was shown in Fig. 6 that the single-span 28 GBaud link EVM improvement using a PSA instead of a PIA has dropped 9.4 dB compared to the single-span 10 GBaud case. Additionally Fig. 9 shows that the dispersion map optimum peak for the single-span 10 GBaud PSA case is much sharper than the 28 GBaud PSA case. For example the 10 GBaud case can tolerate only 2% offset from the optimum dispersion pre-compensation value if 1 dB worse EVM performance is allowed, while the 28 GBaud case can tolerate up to 8% offset. We expect that PSA links with an efficient nonlinearity mitigation performance require a precise dispersion management configuration, while also the third-order dispersion effects increase sensitivity towards the SPM mitigation performance if signal and idler waves are widely spaced.

7. Conclusion

We have presented a numerical dispersion map optimization for one- to four-span dispersion map optimized 28 GBaud PSA links for improved SPM mitigation and compared PSA links with PIA links, such as EDFA amplified links in long-haul transmission simulations at BER = 10^{-3}. The maximum reach of a 28 GBaud PSA link can be extended further by 2.1 times tolerating a total accumulated nonlinear phase shift of 8.8 radians, if four-span optimized dispersion maps are used repeatedly instead of single-span optimized dispersion maps. A significant reach improvement of 6.9 times can be achieved if a four-span optimized PSA link is used instead of an in-line dispersion managed PIA link. However, a reach extension of 4.3 times for a four-span optimized PSA link can be achieved compared to a dispersion unmanaged PIA link with EDC. The multi-span dispersion map optimization for PSA links is beneficial at higher symbol rates where the dispersion length is smaller than a span length $L_D < L_{span}$ and in such conditions a single-span dispersion map optimized PSA link does not provide the best SPM induced nonlinearity mitigation performance anymore. In a WDM PSA system, it is also important to notice the decrease of a SPM mitigation efficiency if the signal and idler waves are separated widely.

Funding

Swedish Research Council (VR) (2015-00535).

Optics EXPRESS

Acknowledgments

The authors would like to acknowledge Benjamin Foo and Kovendhan Vijayan for many fruitful discussions. Egon Astra is acknowledging support from the Study IT in Estonia program and Alfred Ots Scholarship Fund.

References

1. Z. Tong, C. Lundström, P. A. Andrekson, M. Karlsson, and A. Bogris, "Ultralow noise, broadband phase-sensitive optical amplifiers, and their applications," IEEE J. Sel. Topics Quantum Electron. **18**, 1016–1032 (2012).
2. S. L. I. Olsson, B. Corcoran, C. Lundström, T. A. Eriksson, M. Karlsson, and P. A. Andrekson, "Phase-sensitive amplified transmission links for improved sensitivity and nonlinearity tolerance," J. Light. Technol. **33**(3), 710–721 (2015).
3. A. D. Ellis, J. Zhao, and D. Cotter, "Approaching the non-linear Shannon limit," J. Light. Technol. **28**(4), 423–433 (2010).
4. R.-J. Essiambre, G. Kramer, P. J. Winzer, G. J. Foschini, and B. Goebel, "Capacity limits of optical fiber networks," J. Light. Technol. **28**(4), 662–701 (2010).
5. E. Agrell, M. Karlsson, A. R. Chraplyvy, D. J. Richardson, P. M. Krummrich, P. Winzer, K. Roberts, J. K. Fischer, S. J. Savory, B. J. Eggleton, M. Secondini, F. R. Kschischang, A. Lord, J. Prat, I. Tomkos, J. E. Bowers, S. Srinivasan, M. Brandt-Pearce, and N. Gisin, "Roadmap of optical communications," J. Opt., **18**(6), 063002 (2016).
6. S. L. I. Olsson, M. Karlsson, and P. A. Andrekson, "Nonlinear phase noise mitigation in phase-sensitive amplified transmission systems," Opt. Express **23**(9), 11724–11740 (2015).
7. C. M. Caves, "Quantum limits on noise in linear amplifiers," Phys. Rev. D **26**, 1817–1839 (1982).
8. M. Vasilyev, "Distributed phase-sensitive amplification," Opt. Express **13**(19), 7563–7571 (2005).
9. Z. Tong, C. Lundström, P. A. Andrekson, C. J. McKinstrie, M. Karlsson, D. J. Blessing, E. Tipsuwannakul, B. J. Puttnam, H. Toda, and L. Grüner-Nielsen, "Towards ultrasensitive optical links enabled by low-noise phase-sensitive amplifiers," Nat. Photonics **5**(7), 430–436 (2011).
10. M. E. Marhic, P. A. Andrekson, P. Petropoulos, S. Radic, C. Peucheret, and M. Jazayerifar, "Fiber optical parametric amplifiers in optical communication systems," Laser photonics reviews **9**(1), 50–74 (2015).
11. S. L. I. Olsson, H. Eliasson, E. Astra, M. Karlsson, and P. A. Andrekson, "Long-haul optical transmission link using low-noise phase-sensitive amplifiers," Nat. Commun. **9**:2513 (2018).
12. Z. Tong, and S. Radic, "Low-noise optical amplification and signal processing in parametric devices," Adv. Opt. Photonics, **5**(3), 318–384 (2013).
13. X. Liu, A. R. Chraplyvy, P. J. Winzer, R. W. Tkach, and S. Chandrasekhar, "Phase-conjugated twin waves for communication beyond the Kerr nonlinearity limit," Nat. Photonics **7**(7), 560–568 (2013).
14. H. Eliasson, S. L. I. Olsson. M. Karlsson, and P. A. Andrekson, "Comparison between coherent superposition in DSP and PSA for mitigation of nonlinearities in a single-span link," in Proc. European Conference on Optical Communications (ECOC, 2014), paper Mo.3.5.2.
15. H. Eliasson, P. Johannisson, M. Karlsson, and P. A. Andrekson, "Mitigation of nonlinearities using conjugate data repetition," Opt. Express **23**(3), 2392–2402 (2015).
16. S. J. Savory, G. Gavioli, R. I. Killey, and P. Bayvel, "Electronic compensation of chromatic dispersion using a digital coherent receiver," Opt. Express **15**(5), 2120–2126 (2007).
17. V. Curri, P. Poggiolini, A. Carena, and F. Forghieri, "Dispersion compensation and mitigation of nonlinear effects in 111-Gb/s WDM coherent PM-QPSK systems," Photonics Technol. Lett. **20**(17), 1473–1475 (2008).
18. J. K. Fischer, C.-A. Bunge, and K. Petermann, "Equivalent single-span model for dispersion-managed fiber-optic transmission systems," J. Light. Technol. **27**(16), 3425–3432 (2009).
19. A. Cartaxo, N. Costa, and D. Fonseca, "Analysis of optimum dispersion maps for DQPSK systems," in Proc. International Conference on Transparent Optical Networks (ICTON, 2010), paper Mo.D1.1.
20. Y. Frignac and P. Ramantanis, "Average optical phase shift as an indicator of the dispersion management optimization in PSK-modulated transmission systems," Photonics Technol. Lett. **22**(20), 1488–1490 (2010).
21. H. Eliasson, S. L. I. Olsson, M. Karlsson, and P. A. Andrekson, "Mitigation of nonlinear distortion in hybrid Raman/phase-sensitive amplifier links," Opt. Express **24**(2), 888–900 (2016).
22. E. Astra, S. L. I. Olsson, H. Eliasson, and P. A. Andrekson, "Dispersion management for nonlinearity mitigation in two-span 28 GBaud QPSK phase-sensitive amplifier links," Opt. Express **25**(12), 13163–13173 (2017).
23. H. Eliasson, K. Vijayan, B. Foo, S. L. I. Olsson, E. Astra, M. Karlsson, and P. A. Andrekson, "Phase-sensitive amplifier link with distributed Raman amplification," Opt. Express **26**(16), 19854–19863 (2018).
24. E. Astra, H. Eliasson, and P. A. Andrekson, "Four-span dispersion map optimization for improved nonlinearity mitigation in phase-sensitive amplifier links," in Proc. European Conference on Optical Communications (ECOC, 2017), paper P2.SC6.14.
25. Z. Tong, A. Bogris, C. Lundström, C. J. McKinstrie, M. Vasilyev, M. Karlsson, and P. A. Andrekson , "Modeling and measurement of the noise figure of a cascaded non-degenerate phase-sensitive parametric amplifier," Opt. Express **18**(14), 14820–14835 (2010).

Optics EXPRESS

26. R. A. Shafik, S. Rahman, and R. Islam, "On the extended relationships among EVM, BER and SNR as performance metrics," in Proc. 4th International Conference on Electrical and Computer Engineering (ICECE, 2006).
27. A. J. Lowery, "Fiber nonlinearity pre- and post-compensation for long-haul optical links using OFDM," Opt. Express **15**(20), 12965–12970 (2007).
28. R. Sinha, A. K. Garg, and S. Tyagi, "Dispersion compensation techniques: a comprehensive review," Int. J. Electron., Electrical and Computational System **6**(4), 57–61 (2017).
29. L. Gruner-Nielsen, M. Wandel, P. Kristensen, C. Jorgensen, L. V. Jorgensen, B. Edvold, B. Palsdottir, and D. Jakobsen, "Dispersion-compensating fibers," J. Light. Technol. **23**(11), 3566–3579 (2005).
30. F. Ramos, and J. Marti, "Influence of non-ideal chirped fibre grating characteristics on dispersion-compensated analogue optical links in presence of fibre-induced SPM," Electron. Lett. **39**(4), 353–355 (2003).
31. K. Vijayan, H. Eliasson, B. Foo, S. L. I. Olsson, M. Karlsson, and P. A. Andrekson, "Optical bandwidth dependency of nonlinearity mitigation in phase-sensitive amplifier links," in Proc. European Conference on Optical Communications (ECOC, 2018), paper We2.44.
32. R. Tang, P. S. Devgan, V. S. Grigoryan, P. Kumar, and M. Vasilyev , "In-line phase-sensitive amplification of multi-channel CW signals based on frequency nondegenerate four-wave-mixing in fiber," Opt. Express **16**(12), 9046–9053 (2008).
33. K. Vijayan, B. Foo, H. Eliasson, and P. A. Andrekson, "Cross-phase modulation mitigation in WDM transmission systems using phase-sensitive amplifiers," in Proc. European Conference on Optical Communications (ECOC, 2018), paper We3H.4.
34. Z. Tong, C. Lundström, E. Tipsuwannakul, M. Karlsson, and P. A. Andrekson, "Phase-sensitive amplified DWDM DQPSK signals using free-running lasers with 6-dB link SNR improvement over EDFA-based systems," in Proc. European Conference and Exhibition on Optical Communication (ECOC, 2010), paper PDP1.3.